

Rashba Cavity QED: A Route Towards the Superradiant Quantum Phase Transition

Pierre Nataf¹,[✉] Thierry Champel,¹ Gianni Blatter,² and Denis M. Basko¹

¹*Laboratoire de Physique et Modélisation des Milieux Condensés, Université Grenoble Alpes and CNRS, 25 avenue des Martyrs, 38042 Grenoble, France*

²*Institute for Theoretical Physics, ETH Zurich, 8093 Zurich, Switzerland*

 (Received 18 July 2019; revised manuscript received 11 September 2019; published 12 November 2019)

We develop a theory of cavity quantum electrodynamics for a 2D electron gas in the presence of Rashba spin-orbit coupling and perpendicular static magnetic field, coupled to spatially nonuniform multimode quantum cavity photon field. We demonstrate that the lowest polaritonic frequency of the full Hamiltonian can vanish for realistic parameters, achieving the Dicke superradiant quantum phase transition. This singular behavior originates from soft spin-flip transitions possessing a nonvanishing dipole moment at nonzero wave vectors and can be viewed as a static paramagnetic instability.

DOI: [10.1103/PhysRevLett.123.207402](https://doi.org/10.1103/PhysRevLett.123.207402)

The Dicke model, describing an ensemble of identical two-level systems (matter excitations) coupled to a single bosonic (cavity photon) mode, is a prototypical model of cavity quantum electrodynamics (QED) [1]. In the so-called ultrastrong coupling regime [2,3], when the coupling strength (Rabi frequency) becomes comparable to the energy splitting of the two-level system and the photon energy, the Dicke model was shown to exhibit the so-called superradiant quantum phase transition (SQPT) toward a ground state characterized by a finite static average of the photon field [4,5]. The transition was observed [6] in a driven-dissipative quantum simulator of the Dicke model [7,8]; however, the drive effectively introduces a finite temperature [9], so the ground state remains inaccessible. Besides changing the transition critical exponents [9], this irretrievably spoils the low-temperature coherence properties of the superradiant phase, leaving no room [10] for potential quantum applications [11].

To the best of our knowledge, the SQPT has never been observed in a physical matter system coupled to the electromagnetic field, although the ultrastrong coupling regime has been reached in a two-dimensional electron gas (2DEG) placed in a cavity and subject to a perpendicular static magnetic field, so that the matter excitations were represented by the cyclotron resonance [12]. Moreover, a softening of the lowest polaritonic excitation has been observed in this system [13]. Crucially, physical light-matter systems can be described by the Dicke model only in a restricted range of parameters, and the SQPT always lies outside this range. Hence, various extensions of the Dicke model were proposed. The central question is which extensions are physical and how they modify the phase transition. In extended models the SQPT is often prevented by the so-called “no-go” theorems [14–23]. Proposals to circumvent them include systems with magnetic-dipole interactions due to the cavity magnetic fields [24] or its

circuit QED analog with an inductive coupling [11,25]. It has been shown for different physical systems that upon a proper microscopic treatment, the mysterious SQPT assumes the more familiar shape of a crystallization [26], a ferroelectric [27,28] or excitonic insulator [29,30] instability, with the Coulomb interaction playing a crucial role. Moreover, the instability occurred at length scales much shorter than the cavity size, thereby questioning the very role of the transverse cavity field.

In this Letter, we present a model without Coulomb interaction, still exhibiting a SQPT. We consider a 2DEG with Rashba spin-orbit coupling, placed inside an optical cavity, and subject to a perpendicular magnetic field B . In the decoupled 2DEG, the Landau levels can cross at certain values of B corresponding to dipole-allowed excitations with zero energy. The presence of such intrinsic soft excitations greatly enhances the effect of the coupling to the transverse electromagnetic field. We develop a theory of Rashba cavity QED for integer filling factors and show that this coupling leads to further softening of the system and the appearance of “superradiant” phases. Crucially, the instability occurs at a finite wave vector of the cavity field. Even though an effective model including one or few cavity modes may also exhibit a SQPT, for its proper quantitative description many high-energy modes must be included. This instability is of a magnetostatic nature; the resulting “superradiant” phase with a frozen evanescent field is a remote relative of Condon domains of spontaneous magnetization [31–34]. Moreover, it turns out that this instability can also occur without the cavity: the coupling to the free vacuum field appears sufficient.

The model.—Since the effective strength of the light-matter coupling is enhanced if multiple copies of the material system are present [35], we consider n_{QW} identical quantum wells, each hosting a 2DEG with the single-electron Hamiltonian containing a Rashba coupling term [36],

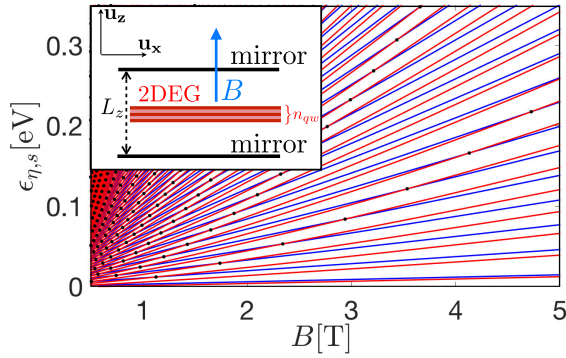


FIG. 1. LL energies $\epsilon_{\eta,s}$ [Eq. (2)] versus B for $\alpha = 0.7$ eV Å and $m^* = 0.02m_0$. The blue (red) curves correspond to $s = +1$ ($s = -1$). The black dots mark the crossings [Eq. (3)]. The inset shows the system geometry.

$$\mathcal{H}_{\text{2DEG}} = \frac{1}{2m^*} (\mathbf{p} + e\mathbf{A}/c)^2 + \alpha [\boldsymbol{\sigma} \times (\mathbf{p} + e\mathbf{A}/c)]_z. \quad (1)$$

Here, $\mathbf{p} = -i(\partial_x, \partial_y)$ is the 2D in-plane electron momentum (we set $\hbar = 1$), m^* is the effective mass, $\boldsymbol{\sigma} = (\sigma_x, \sigma_y, \sigma_z)$ is the vector of Pauli matrices, α is the Rashba spin-orbit coupling constant, $-e < 0$ is the electron charge. Typically, for some existing InSb samples [37], $m^* \simeq 0.02m_0$ (m_0 being the free electron mass), $\alpha \simeq 0.7$ eV Å. Finally, the vector potential $\mathbf{A} = \mathbf{A}^{\text{ext}} + \mathbf{A}^{\text{cav}}$ consists of two parts.

First, $\mathbf{A}^{\text{ext}}(\mathbf{r}) = (-By, 0, 0)$ corresponds to the external magnetic field B , applied perpendicularly to the 2DEG plane (in the z direction). The resulting single-particle spectrum consists of Landau levels (LLs) with energies

$$\epsilon_{\eta,s} = \omega_c \left(\eta + \frac{s}{2} \sqrt{1 + 8\eta\gamma^2} \right), \quad (2)$$

where $\eta = 0, 1, 2, \dots$ is the LL index, $s = \pm 1$ for $\eta \geq 1$ and $s = 1$ for $\eta = 0$ is what remains of the spin index, $\omega_c = eB/(m^*c)$ is the cyclotron frequency, and $\gamma \equiv \alpha m^* l_B$ with $l_B \equiv (eB/c)^{-1/2}$ being the magnetic length. In Fig. 1, we show $\epsilon_{\eta,s}$ for parameters consistent with InSb [37]; the spectrum exhibits crossings between LLs (η_1, s) and $(\eta_2, -s)$ satisfying the conditions [38] $|\eta_1 - \eta_2| > 1$ and

$$\alpha^2 = \frac{\eta_1 + \eta_2 - \sqrt{4\eta_1\eta_2 + 1}}{2(m^*l_B)^2}. \quad (3)$$

Levels with the same s never cross. Each LL has a degeneracy $L_x L_y / (2\pi l_B^2)$ where $L_x L_y$ is the sample area. We assume to be at zero temperature, at a fixed electron density n_e , and at B corresponding to an integer filling factor $\nu \equiv 2\pi l_B^2 n_e$. Indeed, the SQPT is associated with a reconstruction of the nondegenerate ground state in a gapped system. Lifting the ground state degeneracy at fractional fillings represents a totally different problem.

The vector potential $\mathbf{A}^{\text{cav}}(\mathbf{r})$ of the cavity field is defined by the mode expansion, determined by the cavity shape. For simplicity, we consider a perfect metallic cavity with dimensions $L_x \gg L_z \gg L_y$, filled by a material with a dielectric constant ϵ . Then, one can consider only resonator modes with wave vectors $\mathbf{q} = (q_x, 0, q_z)$, where q_x is continuous and $q_z = \pi n_z / L_z$, $n_z = 1, 2, 3, \dots$. The corresponding mode frequencies are $\omega_{q_x, n_z}^{\text{cav}} = (c/\sqrt{\epsilon}) \sqrt{q_x^2 + q_z^2}$. The cavity vector potential then reads [39,40]

$$\mathbf{A}^{\text{cav}}(\mathbf{r}) = \sum_{q_x, n_z} \sqrt{\frac{4\pi}{L_x L_y L_z \epsilon \omega_{q_x, n_z}}} \mathbf{u}_y \sin \frac{n_z \pi z}{L_z} \times (a_{q_x, n_z} e^{iq_x x} + a_{q_x, n_z}^\dagger e^{-iq_x x}), \quad (4)$$

where a_{q_x, n_z}^\dagger (a_{q_x, n_z}) is the photon creation (annihilation) operator and \mathbf{u}_y is the unit vector in the y direction. We assume the whole 2DEG sample with n_{QW} quantum wells to be much thinner than L_z and placed at $z = L_z/2$ (Fig. 1, inset). Then, what enters Eq. (1), is $\mathbf{A}^{\text{cav}}(z = L_z/2)$ and the modes with even n_z are decoupled.

Polaritons and instability.—The SQPT is signaled by the vanishing of the lowest polariton frequency. The polariton modes—the excitations of the coupled 2DEG-cavity system—can be found by several methods. For example, similarly to Ref. [40] for the same problem without spin-orbit coupling, one writes the 2DEG many-body Hamiltonian in terms of approximately bosonic operators for inter-LL excitations; then the full 2DEG and cavity Hamiltonian becomes bilinear and is diagonalized by the Bogoliubov transformation. Alternatively, one can write the action for coupled electron and photon fields, integrate out the electrons, and expand the resulting bosonic action to the second order in \mathbf{A}^{cav} . Both (rather standard) calculations are given in the Supplemental Material [41], and their equivalence is checked explicitly.

As a result, the polariton frequencies are given by the solution of the following equation:

$$\frac{c}{2\pi} \sqrt{c^2 q_x^2 - \epsilon \omega^2} \coth \frac{L_z \sqrt{q_x^2 - \epsilon \omega^2 / c^2}}{2} = -Q_{yy}(q_x, \omega), \quad (5)$$

where $Q_{yy}(q_x, \omega)$ is the susceptibility determining the linear response $j_y = Q_{yy}(\delta A_y/c) e^{iq_x x - i\omega t}$ of the 2D electron current density j_y to a perturbing vector potential $\delta \mathbf{A}$ on top of \mathbf{A}^{ext} included in the unperturbed system, $\mathbf{A} = \mathbf{A}^{\text{ext}} + \delta \mathbf{A} e^{iq_x x - i\omega t}$. The susceptibility consists of two contributions, the diamagnetic one and the sum over all inter-LL transitions in all quantum wells,

$$Q_{yy}(q_x, \omega) = \frac{n_{\text{QW}} n_e e^2}{m^*} \left(1 - \frac{\omega_c}{\nu} \sum_{\ell \leq \nu < \ell'} \frac{\omega_{\ell' \ell}^{\text{LL}} [g_{q_x}^{\ell'}]^2}{(\omega_{\ell' \ell}^{\text{LL}})^2 - \omega^2} \right). \quad (6)$$

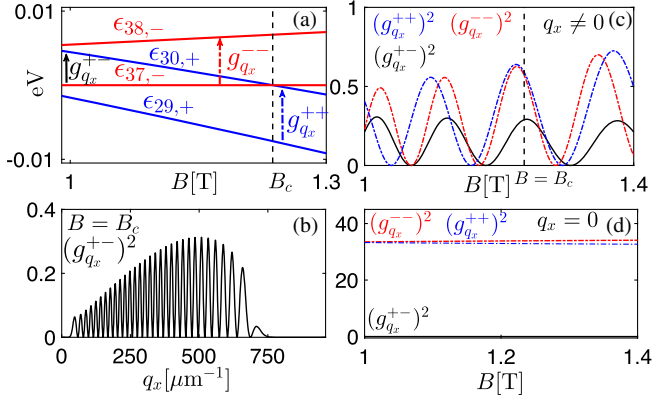


FIG. 2. (a) LL energies $\epsilon_{29,+}$, $\epsilon_{30,+}$, $\epsilon_{37,-}$, $\epsilon_{38,-}$ [Eq. (2)] versus B for the parameters of Fig. 1. The gap closes between the states $|37, -\rangle$ and $|30, +\rangle$ at $B_c \simeq 1.23721$ T. (b) The spin-flip dipole squared $(g_{q_x}^{+-})^2 \equiv (g_{q_x}^{30+,37-})^2$ [Eq. (7)] versus q_x at $B = B_c$. At $q_x = 0$, it vanishes by gauge invariance. When q_x increases, it oscillates and takes nonzero values, opening the possibility of a diverging oscillator strength proportional to $(g_{q_x}^{+-})^2 / (\epsilon_{30,+} - \epsilon_{37,-})$. Finally, we plot $(g_{q_x}^{+-})^2$, $(g_{q_x}^{++})^2$, and $(g_{q_x}^{--})^2$ versus B for $q_x = 4 \times 10^8 \text{ m}^{-1}$ in (c) and $q_x = 0$ in (d).

Here, the LL indices $(\eta, s) \equiv \ell$ are combined into a single label, ordered according to the LL energies ϵ_ℓ , Eq. (2), so that LLs with $\ell \leq \nu$ are filled, and those with $\ell > \nu$ are empty. The transition energy $\omega_{\ell'\ell}^{\text{LL}} \equiv \epsilon_{\ell'} - \epsilon_\ell$, and the reduced coupling constants $g_{q_x}^{\ell'\ell}$ (dipole matrix elements) are defined as

$$g_{q_x}^{\ell'\ell} = -\sqrt{2}\gamma(\sin\theta_{\ell'}\cos\theta_\ell\Theta_{\eta'}^\eta - \cos\theta_{\ell'}\sin\theta_\ell\Theta_{\eta'}^{\eta-1}) + \sin\theta_{\ell'}\sin\theta_\ell\left(\sqrt{\eta-1}\Theta_{\eta'}^{\eta-2} - \sqrt{\eta}\Theta_{\eta'}^{\eta-1}\right) + \cos\theta_{\ell'}\cos\theta_\ell\left(\sqrt{\eta}\Theta_{\eta'}^{\eta-1} - \sqrt{\eta+1}\Theta_{\eta'}^{\eta+1}\right), \quad (7)$$

where $\tan\theta_l = [-1 + s\sqrt{1+8\eta\gamma^2}]/(\sqrt{8\eta\gamma})$, and the overlap function $\Theta_{n_2}^{n_1}$ containing the q_x dependence is given by

$$\Theta_{n_2}^{n_1} = \sqrt{\frac{m!}{M!}} e^{-\xi/2} \xi^{(M-m)/2} L_m^{(M-m)}(\xi) S^{n_2-n_1}, \quad (8)$$

with $L_m^{(M-m)}(\xi)$ the generalized Laguerre polynomial of $\xi \equiv l_B^2 q_x^2 / 2$, $S = \text{sgn}[q_x(n_2 - n_1)]$, $m = \min\{n_1, n_2\}$, and $M = \max\{n_1, n_2\}$. Since at $q_x = 0$ we have $\Theta_{n_2}^{n_1} = \delta_{n_1, n_2}$, the reduced coupling constants $g_{q_x=0}^{\ell'\ell}$ are nonzero only between consecutive LLs, $\eta' = \eta \pm 1$, with no restriction on s . At finite q_x , this selection rule is relaxed.

Equations (5)–(8) represent the main analytical result of this Letter. Note that in Eq. (5) all information about the cavity is on the left-hand side (lhs), while all information about the 2DEG is on the right. At $\omega = 0$ (at the sought SQPT) the lhs is proportional to c^2 which is much larger

than any velocity scale occurring in a typical solid. Moreover, when $\omega = 0$, the second term on the right-hand side (rhs) of Eq. (6) is nothing but the total sum of the oscillator strengths $|g_{q_x}^{\ell'\ell}|^2 / \omega_{\ell'\ell}^{\text{LL}}$, which is the fundamental quantum optics quantity that determines the occurrence of the SQPT in multilevel systems [19]. It diverges at the level crossing, balancing the large c^2 factor on the lhs and allowing a solution to Eq. (5).

The key reason is that for the spin-flip transitions at $q_x \neq 0$, the dipoles $g_{q_x}^{\ell'\ell}$ can be nonzero even at a crossing between $\epsilon_{\ell'}$ and ϵ_ℓ , opening the possibility of a diverging oscillator strength, as illustrated in Fig. 2. This is in sharp contrast with what happens at $q_x = 0$. Indeed, for a generic single-electron Hamiltonian \mathcal{H} , after the minimal coupling replacement of the electron momentum $\mathbf{p} \rightarrow \mathbf{p} + (e/c)\mathbf{A}_{\text{cav}}$, where \mathbf{A}_{cav} is the uniform cavity field, the matrix element of the linear light-matter coupling term between two arbitrary eigenstates $|1\rangle$, $|2\rangle$ of \mathcal{H} , is proportional to that of the electron velocity $\mathbf{v} = \partial\mathcal{H}/\partial\mathbf{p} = i[\mathcal{H}, \mathbf{r}]$, so that $\mathbf{v}_{12} = \langle 1 | [\mathcal{H}, \mathbf{r}] | 2 \rangle = (\epsilon_1 - \epsilon_2) \langle 1 | \mathbf{r} | 2 \rangle$. At the crossing $\epsilon_1 - \epsilon_2$ vanishes, so both the velocity matrix element \mathbf{v}_{12} and the oscillator strength $\propto |\mathbf{v}_{12}|^2 / (\epsilon_1 - \epsilon_2)$ vanish. Crucially, this argument does not apply to spatially nonuniform fields.

From a different perspective, gauge invariance imposes a constraint on $Q_{yy}(q_x, \omega)$: a physical quantity (current) cannot respond to a static spatially homogeneous vector potential, thus $Q_{yy}(0, 0) = 0$ (see S3 in [41] for details). This prohibits the instability at $q_x = 0$; models or approximations violating this constraint can give wrong results. $Q_{yy}(0, 0) = 0$ implies a cancellation between the two terms in Eq. (6). This cancellation is usually ensured by sum rules such as the Thomas-Reiche-Kuhn sum rule [14,17–21,23]. Here, we have checked numerically that $Q_{yy}(0, 0) = 0$.

Figure 3(a) shows the two sides of Eq. (5) at $\omega = 0$ as functions of the cavity field wave vector q_x , and six values of $q_x > 0$ (vertical dashed lines) when $\omega = 0$ is a solution. In Fig. 3(b), we plot the solution of Eq. (5) for ω , which indeed vanishes at the indicated values of q_x . This curve shows that the system is unstable. It cannot be interpreted as the excitation frequency for parameter values corresponding to the superradiant phase, since the ground state is reconstructed, and an additional mean-field term should be introduced into Hamiltonian (1). This term spontaneously breaks the translational symmetry, so q_x is not a good quantum number anymore. The spatial profile of the symmetry breaking term must be determined from self-consistent mean-field equations, which is beyond the scope of this Letter. In the inset of Fig. 3(a), we plot the two sides of Eq. (5) at $\omega = 0$ versus B for given q_x , for $n_{\text{QW}} = 1$ and $n_{\text{QW}} = 10^3$. Essentially, we exploit a divergence appearing around level crossings to make Eq. (5) have a solution, and then use large n_{QW} to extend the superradiant region.

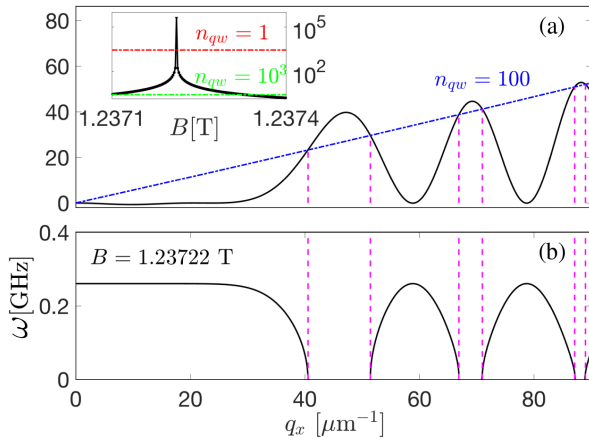


FIG. 3. (a) The rhs (the solid black curve) and the lhs (the dash-dotted blue curve) of Eq. (5) at $\omega = 0$ divided by $(n_{\text{QW}} n_e e^2 / m^*)$, plotted versus q_x at $B = 1.23722$ T [which exceeds B_c , cf. Fig. 2(a)] for $\alpha = 0.7$ eV \AA , $m^* = 0.02m_0$, $\nu = 67$, $L_z = 20$ μm , $\varepsilon = 10$, $n_{\text{QW}} = 100$. Their crossings, shown by the vertical dashed lines, give solutions of Eq. (5) for q_x at $\omega = 0$. Inset: the same quantities plotted versus B for $q_x = 4.8 \times 10^7$ m^{-1} , where the red (respectively, green) curve corresponds to $n_{\text{QW}} = 1$ (respectively, $n_{\text{QW}} = 1000$). (b) Solution of Eq. (5) for ω , vanishing at the indicated q_x , for $n_{\text{QW}} = 100$.

Figure 4 shows the instability regions in the (α, q_x) plane for fixed B and ν . They appear for $q_x \neq 0$ and for α close to those given by Eq. (3) for some integers $\eta_1 \neq \eta_2$, $\eta_1 + \eta_2 = \nu$, shown by dashed red lines in Fig. 4. The characteristic width $\Delta\alpha$ of the “superradiant” regions on the phase diagram can be estimated as (Supplemental Material, S4 [41])

$$\Delta\alpha \sim \frac{1}{\nu^2} \frac{n_{\text{QW}} n_e e^2}{(m^* c)^2}, \quad (9)$$

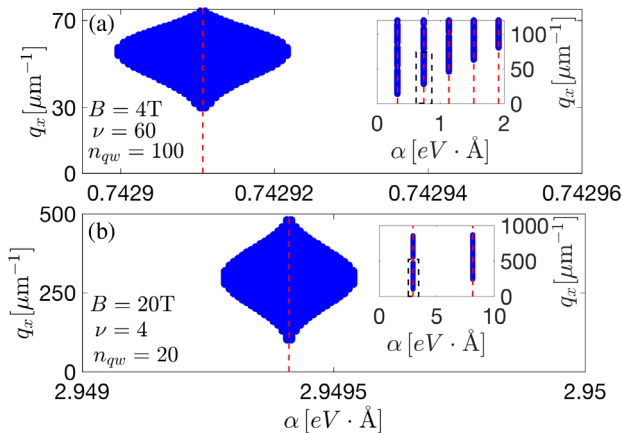


FIG. 4. Instability regions (in blue) in the parameter plane (α, q_x) for different B , ν , and n_{QW} , also displayed for a wider range of parameters in the insets. Dashed red lines show values of α which produce a level crossing [Eqs. (2), (3)]. The instability occurs around these crossings. (a) $B = 4$ T, $\nu = 60$, and $n_{\text{QW}} = 100$; (b) $B = 20$ T, $\nu = 4$, and $n_{\text{QW}} = 20$.

and the typical scale of q_x is given by the inverse cyclotron radius $(\sqrt{\nu} l_B)^{-1}$. The superradiant regions are very narrow; this happens because the mechanism for the instability can be traced to the magnetostatic interaction, as discussed below. Typically, one arrives at the Dicke model assuming the light-matter coupling via the cavity electric field. However, this electric field, $\propto \partial \mathbf{A}_{\text{cav}} / \partial t$, vanishes at $\omega = 0$. The remaining magnetic interaction is intrinsically weak. These simple physical arguments are not obvious from the equations.

From Eq. (9) and Fig. 4 we see that small filling factors are favoring the superradiant phase. This is in stark contrast to the condition of $\nu \gg 1$ formulated in Ref. [40] to achieve the ultrastrong coupling regime because the SQPT obtained here is determined by the magnetic coupling and not the electric one.

Finally, it is meaningful to consider the limit $L_z \rightarrow \infty$ in Eq. (5), corresponding to simply removing the mirrors. Moreover, the smallest unstable $q_x \approx 40$ μm^{-1} in Fig. 3(b) is already deep in this limit, $\coth(q_x L_z / 2) \approx 1$. In fact, the same instability can be obtained by considering just the magnetostatic energy of a 2DEG in a uniform magnetic field. Normally, such a 2DEG has a uniform magnetization. However, it may be energetically advantageous to spontaneously develop an additional spatially modulated magnetization, which produces a space-dependent evanescent magnetic field. This, in turn, couples to the magnetization, lowering the total energy of the 2DEG and the field. The criterion for this paramagnetic instability (Supplemental Material, S5 [41]) coincides with Eq. (5) at $\omega = 0$, $L_z \rightarrow \infty$. The resulting modulated magnetization pattern is analogous to the so-called Condon domains [31–34]. Indeed, such a domain structure has the characteristics of the superradiant phase: the magnetic field produced by the domains corresponds to a nonzero expectation value of the photon field $\langle a_{q_x, n_z} \rangle$. Note that no-go theorems for inhomogeneous field configurations were established for a collection of nonmagnetic [15,21] or diamagnetic [16] atoms excluding a paramagnetic instability.

Conclusions and outlook.—We proved that the SQPT can be reached in a cavity QED system with Rashba spin-orbit coupling and nonuniform cavity fields due to the singularity of spin-flip transitions, for which the spin-flip dipole at $q_x \neq 0$ can be nonzero even if the transition energy vanishes. Consequently, the SQPT must occur close to LLs energy crossings and requires relatively fine tuning of B and n_e , as well as large n_{QW} . We have shown that the SQPT can be viewed as a static paramagnetic instability of the 2DEG, the static cavity field corresponding to the evanescent magnetic field induced by a spatially modulated 2DEG magnetization. Moreover, the presence of the cavity is not necessary: the SQPT can also happen via the coupling to the free vacuum field.

The microscopic model we studied in this Letter has the minimal number of ingredients necessary to produce the

SQPT. We adopted a simplified description of the cavity field, focusing on the transverse electric modes propagating in the x direction; a more realistic description [44–46] may change the results quantitatively. To make a connection with state-of-the-art experiments [12,13], other ingredients must be introduced. Zeeman coupling is likely to enhance the effect since the spin contribution to the 2DEG magnetic susceptibility is usually paramagnetic. Coulomb interaction is also likely to further soften the excitations due to the excitonic effect. Very important is the disorder which lifts the LL degeneracy and broadens the cyclotron resonance. Coherent state based methods successfully describe the local density of states in a 2DEG with smooth disorder in a strong magnetic field [38,47]; the effect of smooth disorder on the inter-LL transitions remains an open problem. Effects of strain, as well as mixing between bands with different spins, which both influence the amplitude and the nature of the Rashba coupling [48–50], could also be studied. Adapting our calculations to other cavities, where an additional geometric factor can enhance the light-matter interaction [51], could also be useful. Finally, in this Letter, we focused on the instability, leaving aside the study of the superradiant phase itself, a topic that deserves future investigation as well.

We acknowledge fruitful discussions with Tobias Wolf, Matteo Biondi, Jérôme Faist, Giacomo Scalari, Janine Keller, Maksym Myronov, Rai Moriya, Takaaki Koga, Roland Winkler, Cristiano Ciuti and David Hagenmüller.

-
- [1] R. H. Dicke, *Phys. Rev.* **93**, 99 (1954).
 [2] C. Ciuti, G. Bastard, and I. Carusotto, *Phys. Rev. B* **72**, 115303 (2005).
 [3] P. Forn-Díaz, L. Lamata, E. Rico, J. Kono, and E. Solano, *Rev. Mod. Phys.* **91**, 025005 (2019).
 [4] K. Hepp and E. H. Lieb, *Ann. Phys. (N.Y.)* **76**, 360 (1973).
 [5] C. Emary and T. Brandes, *Phys. Rev. E* **67**, 066203 (2003).
 [6] K. Baumann, C. Guerlin, F. Brennecke, and T. Esslinger, *Nature (London)* **464**, 1301 (2010).
 [7] F. Dimer, B. Estienne, A. S. Parkins, and H. J. Carmichael, *Phys. Rev. A* **75**, 013804 (2007).
 [8] F. Damanet, A. J. Daley, and J. Keeling, *Phys. Rev. A* **99**, 033845 (2019).
 [9] P. Kirton, M. M. Roses, J. Keeling, and E. G. Dalla Torre, *Adv. Quantum Technol.* **2**, 1800043 (2019).
 [10] K. R. Brown, *Phys. Rev. A* **76**, 022327 (2007).
 [11] P. Nataf and C. Ciuti, *Phys. Rev. Lett.* **107**, 190402 (2011).
 [12] G. Scalari, C. Maissen, D. Turčinková, D. Hagenmüller, S. De Liberato, C. Ciuti, C. Reichl, D. Schuh, W. Wegscheider, M. Beck, and J. Faist, *Science* **335**, 1323 (2012).
 [13] J. Keller, G. Scalari, F. Appugliese, C. Maissen, J. Haase, M. Failla, M. Myronov, D. R. Leadley, J. Lloyd-Hughes, P. Nataf, and J. Faist, *arXiv:1708.07773*.
 [14] K. Rzażewski, K. Wódkiewicz, and W. Żakowicz, *Phys. Rev. Lett.* **35**, 432 (1975).
 [15] I. Białynicki-Birula and K. Rzażewski, *Phys. Rev. A* **19**, 301 (1979).
 [16] K. Gawędzki and K. Rzażewski, *Phys. Rev. A* **23**, 2134 (1981).
 [17] P. Nataf and C. Ciuti, *Nat. Commun.* **1**, 72 (2010).
 [18] Y. Todorov and C. Sirtori, *Phys. Rev. B* **85**, 045304 (2012).
 [19] M. Hayn, C. Emary, and T. Brandes, *Phys. Rev. A* **86**, 063822 (2012).
 [20] L. Chirrolli, M. Polini, V. Giovannetti, and A. H. MacDonald, *Phys. Rev. Lett.* **109**, 267404 (2012).
 [21] M. Bamba and T. Ogawa, *Phys. Rev. A* **90**, 063825 (2014).
 [22] E. Rousseau and D. Felbacq, *Sci. Rep.* **7**, 11115 (2017).
 [23] G. M. Andolina, F. M. D. Pellegrino, V. Giovannetti, A. H. MacDonald, and M. Polini, *Phys. Rev. B* **100**, 121109(R) (2019).
 [24] J. M. Knight, Y. Aharonov, and G. T. C. Hsieh, *Phys. Rev. A* **17**, 1454 (1978).
 [25] P. Nataf and C. Ciuti, *Phys. Rev. Lett.* **104**, 023601 (2010).
 [26] A. Vukics, T. Griebner, and P. Domokos, *Phys. Rev. A* **92**, 043835 (2015).
 [27] J. Keeling, *J. Phys. Condens. Matter* **19**, 295213 (2007).
 [28] D. De Bernardis, T. Jaako, and P. Rabl, *Phys. Rev. A* **97**, 043820 (2018).
 [29] F. M. D. Pellegrino, V. Giovannetti, A. H. MacDonald, and M. Polini, *Nat. Commun.* **7**, 13355 (2016).
 [30] G. Mazza and A. Georges, *Phys. Rev. Lett.* **122**, 017401 (2019); the mistake of this Letter is to conclude that the excitonic instability is accompanied by spontaneous generation of a static and spatially uniform average value of the vector potential, as pointed out in Ref. [23].
 [31] D. Shoenberg, *Magnetic Oscillations in Metals* (Cambridge University Press, Cambridge, England, 1984).
 [32] R. S. Markiewicz, M. Meskoob, and C. Zahopoulos, *Phys. Rev. Lett.* **54**, 1436 (1985).
 [33] J. J. Quinn, *Nature (London)* **317**, 389 (1985).
 [34] A. Gordon, M. A. Itskovsky, I. D. Vagner, and P. Wyder, *Phys. Rev. Lett.* **81**, 2787 (1998).
 [35] C. Weisbuch, M. Nishioka, A. Ishikawa, and Y. Arakawa, *Phys. Rev. Lett.* **69**, 3314 (1992).
 [36] Y. A. Bychkov and É. I. Rashba, *Pis'Ma Zh. Eksp. Teor. Fiz.* **39**, 66 (1984) [*JETP Lett.* **39**, 78 (1984)].
 [37] S. Becker, M. Liebmann, T. Mashoff, M. Pratzner, and M. Morgenstern, *Phys. Rev. B* **81**, 155308 (2010).
 [38] D. Hernangómez-Pérez, J. Ulrich, S. Florens, and T. Champel, *Phys. Rev. B* **88**, 245433 (2013).
 [39] K. Kakazu and Y. S. Kim, *Phys. Rev. A* **50**, 1830 (1994).
 [40] D. Hagenmüller, S. De Liberato, and C. Ciuti, *Phys. Rev. B* **81**, 235303 (2010).
 [41] See Supplemental Material at <http://link.aps.org/supplemental/10.1103/PhysRevLett.123.207402> for the details of the different calculations, which includes Refs. [42,43].
 [42] P. Nataf, A. Baksic, and C. Ciuti, *Phys. Rev. A* **86**, 013832 (2012).
 [43] A. Baksic and C. Ciuti, *Phys. Rev. Lett.* **112**, 173601 (2014).
 [44] X. Li, M. Bamba, Q. Zhang, S. Fallahi, G. C. Gardner, W. Gao, M. Lou, K. Yoshioka, M. J. Manfra, and J. Kono, *Nat. Photonics* **12**, 324 (2018).

- [45] J. Chen, A. A. Zadorozhko, and D. Konstantinov, *Phys. Rev. B* **98**, 235418 (2018).
- [46] M. Bamba, X. Li, and J. Kono, *Proc. SPIE Int. Soc. Opt. Eng.* **XXIII**, 1091605 (2019).
- [47] T. Champel and S. Florens, *Phys. Rev. B* **80**, 161311(R) (2009).
- [48] R. Winkler, M. Merkler, T. Darnhofer, and U. Rössler, *Phys. Rev. B* **53**, 10858 (1996).
- [49] R. Winkler, *Phys. Rev. B* **62**, 4245 (2000).
- [50] R. Moriya, K. Sawano, Y. Hoshi, S. Masubuchi, Y. Shiraki, A. Wild, C. Neumann, G. Abstreiter, D. Bougeard, T. Koga, and T. Machida, *Phys. Rev. Lett.* **113**, 086601 (2014).
- [51] C. Maissen, G. Scalari, F. Valmorra, M. Beck, J. Faist, S. Cibella, R. Leoni, C. Reichl, C. Charpentier, and W. Wegscheider, *Phys. Rev. B* **90**, 205309 (2014).